

Final report

The role of NMNAT-1 in cancer cell chemosensitivity (PD 116845)

Introduction

Osteosarcoma is the most prevalent neoplasm of the bone in children and adolescents, with approximately 850,000 cases reported each year in the US. Treatment of osteosarcoma usually begins with neoadjuvant chemotherapy followed by surgical removal of the primary tumor and metastases (typically localized to the lungs). Agents used for osteosarcoma chemotherapy include cisplatin, methotrexate, and doxorubicin. The rather poor therapeutic responsiveness indicates that new treatment modalities are clearly needed to improve the disease-free survival of osteosarcoma patients.

Neoplastic transformation is accompanied by fundamental rearrangements of metabolic pathways. A key hallmark of cancer metabolism is the reliance of tumor cells on glycolysis, even if oxygen is available (aerobic glycolysis, also known as the Warburg effect) [1]. NAD⁺ is a central metabolite of energy production that serves as an electron carrier in glycolysis and the TCA cycle. In addition to its role as a metabolic cofactor, NAD also has signaling roles [2].

Maintaining the nuclear NAD concentration is essential, regarding the activity of nuclear NAD dependent enzymes, like PARP1 and SIRT1, which enzymes require much more NAD, than redox processes. PARP1 regulates diverse cellular processes, like DNA repair, replication, or cell migration [3]. But, based on the synthetic lethality paradigm, PARP1 is the primary target for a novel cancer therapeutic modality [4]. Cancer cells with mutations in BRCA1/2 genes are more sensitive to PARPi compounds.

NAD metabolism can also be targeted for cancer therapy. Certain enzymes of NAD-synthesis are already used as target in trials against cancer [5]. Since inhibitor molecules are available for NAMPT, our knowledge on the targetability of NAD synthesis for cancer therapy comes from experiments with the NAMPT inhibitor compounds, FK866 and GMX1777. Although these drug candidates efficiently kill cancer cells, they also show some toxicity in non-transformed cells. In clinical trials, these drugs were relatively well-tolerated and displayed acceptable safety profiles [6]. Nicotinamide mononucleotide adenylyltransferase-1 (NMNAT1) is a nuclear enzyme plays a key role in nuclear NAD⁺ metabolism by catalyzing the final step by forming NAD from NMN and ATP. It is reported, that the expression of (NMNAT-1) is induced upon genotoxic stimulus [7], which may show the role of the enzyme in tumor cell survival. The physical interaction between NMNAT1 and PARP1 during transcription is also discovered [8]. In our current study, we aimed to investigate the role of NMNAT1 in cancer cell chemosensitivity.

Results

The possible consequences of NMNAT-1 deletion in tumors are still controversial, it may contribute to transformation by increasing rRNA synthesis [7], but may also increase sensitivity to DNA damage [7]. So far there is no direct evidence that PARP-1 and NMNAT-1 may interact in cancer cell chemosensitivity, but silencing of NMNAT-1 was reported to delay the repair of single strand DNA breaks [7]. Limited information is available about the NMNAT1 expression of tumor cell lines.

Eleven human tumor cell lines were tested for NMNAT-1 expression (Fig 1A). However, NMNAT-1 was expressed in all the tested cell lines, but in different levels. In comparison with the average expression, A431 shows a significantly higher mRNA expression level, while significantly lower expression was detected in A549, Capan2, MCF7 and HepG2 cell lines. U2OS, with an average NMNAT1 expression was selected for further investigation. Induction of NMNAT1 expression was shown upon doxorubicin treatment [7]. Our data show, that DNA-targeting antitumor treatment not only with doxorubicin, but also with cisplatin shows a significant elevation in NMNAT1 expression in U2OS cell line (Fig 1B). As NMNAT1 expression increased in both cases, it may be hypothesized, that NMNAT1 may have an important role in cell survival.

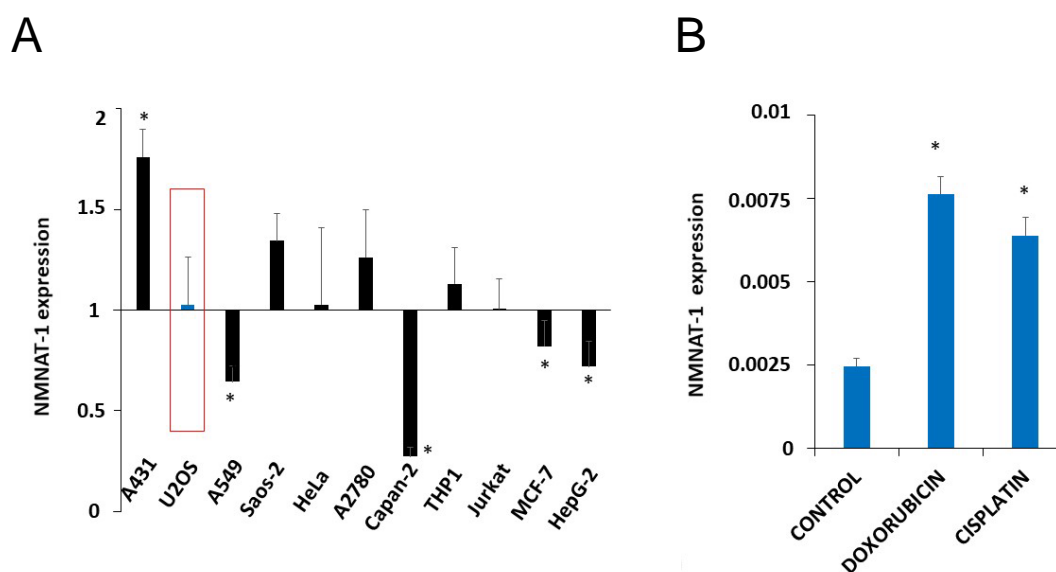


Fig 1. NMNAT1 expression and induction

Basal relative expression of NMNAT1 was determined in eleven human tumor cell lines at mRNA level. The position of x axis shows the average expression level of the tested cell lines (A). U2OS cell line was chosen for further investigation. Induction of NMNAT1 expression in U2OS cell line was examined by RT-QPCR method, at 24 hours after the indicated treatments (B).

The following experiments were performed with cisplatin treatment. Viability of U2OS cells was tested with a concentration series of cisplatin (Fig2A). Cisplatin caused a concentration-dependent decrease in viability, 6.25 $\mu\text{g}/\text{mL}$ was used in the following experiments. As NMNAT1 takes part in both salvage and *de novo* synthesis of NAD [9], a total NAD level was determined in control, and cisplatin treated samples. No significant change was detected (FIG 2B).

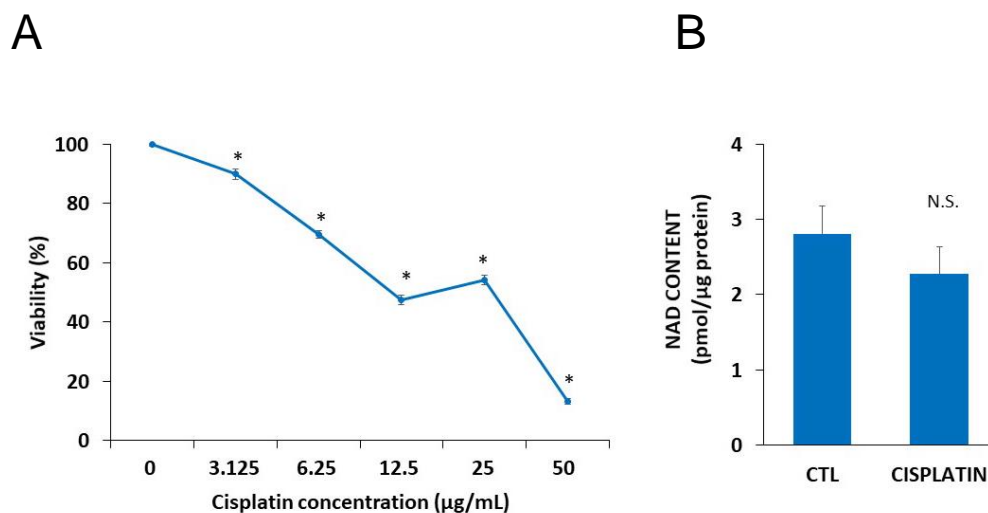


Fig 2. The effect of cisplatin on viability and NAD content

Calcein AM assay was tested the concentration-dependent cytotoxic effect of cisplatin (3.125-50 $\mu\text{g}/\text{mL}$) on U2OS cells after 24 hours of cisplatin treatment (A). Total NAD content was measured from cell lysates after 24 hours of cisplatin treatment and normalized to protein content (B). Data is expressed in means \pm SEM (n = 3). *P < 0.05; **P < 0.01; ***P < 0.001.

As NMNAT1 lacks a specific inhibitor, we set out to eliminate the gene. Crispr-Cas9 technique was applied for genome editing. Successfully transfected cells were selected by puromycin resistance. In the second round, cells were sorted for RFP signal and single cell colonies were generated. All transfected clones lack in NMNAT1 expression at mRNA level (Fig 3A). Clone, 1B6 was selected for further investigation. NMNAT1 protein expression was detected with Western blot (Fig 3B) in the WT cell line, not any sign of NMNAT1 could be detected in the KO cell line.

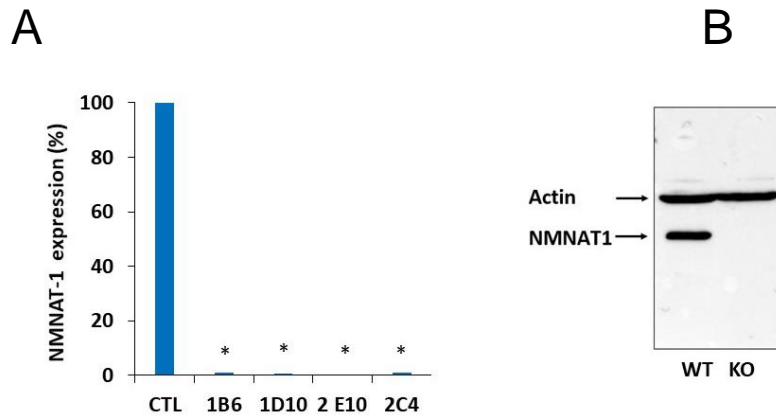


Fig 3. Generation of an NMNAT1 knockout cell line

NMNAT1 knockout cell line was generated with CRISPR-CAS9 system. Puromycin resistant cells were sorted and single cell colonies were grown. NMNAT1 mRNA levels were measured with RT-QPCR method in each colonies. Results are expressed as a percentage of NMNAT1 expression of the wild type U2OS cell line (A). Clone 1B6 was chosen for further investigation. NMNAT1 expression was determined at protein level with Western blot method from cell lysates of wild type U2OS and the 1B6 clone (B).

In the next part of our recent work, characteristics of the new, NMNAT-1 KO cell line were determined. No significant change was detected in cell viability with calcein AM assay (Fig 4A), however the clonogenic activity of the KO cells was significantly decreased (Fig 4B).

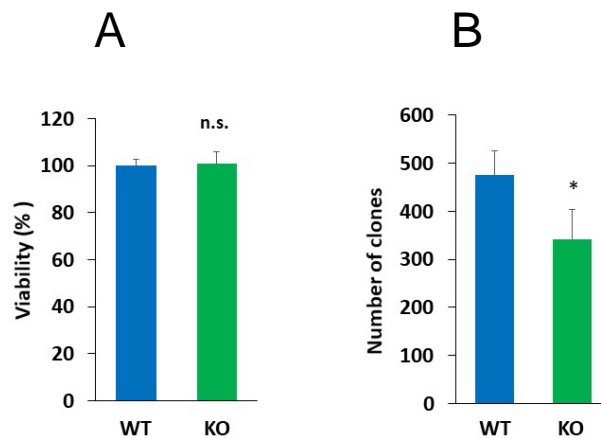


Fig 4. Characterization of the NMNAT1 KO cell line: viability and proliferation

Viability was measured with Calcein AM viability assay (A). Clonogenic activity was determined in a conventional clonogenic assay, run for 6 days (B). Data is expressed in means \pm SEM (n = 3). *P < 0.05; **P < 0.01; ***P < 0.001.

Morphological properties of wild type and NMNAT1 knockout cells were analyzed. HCA method was used for quantification. A significant reduction was detected in the size of nucleus and also in the size of the whole cell (Fig 5). The nuclear and cellular roundness is also significantly different in KO cells, compared to WT ones.

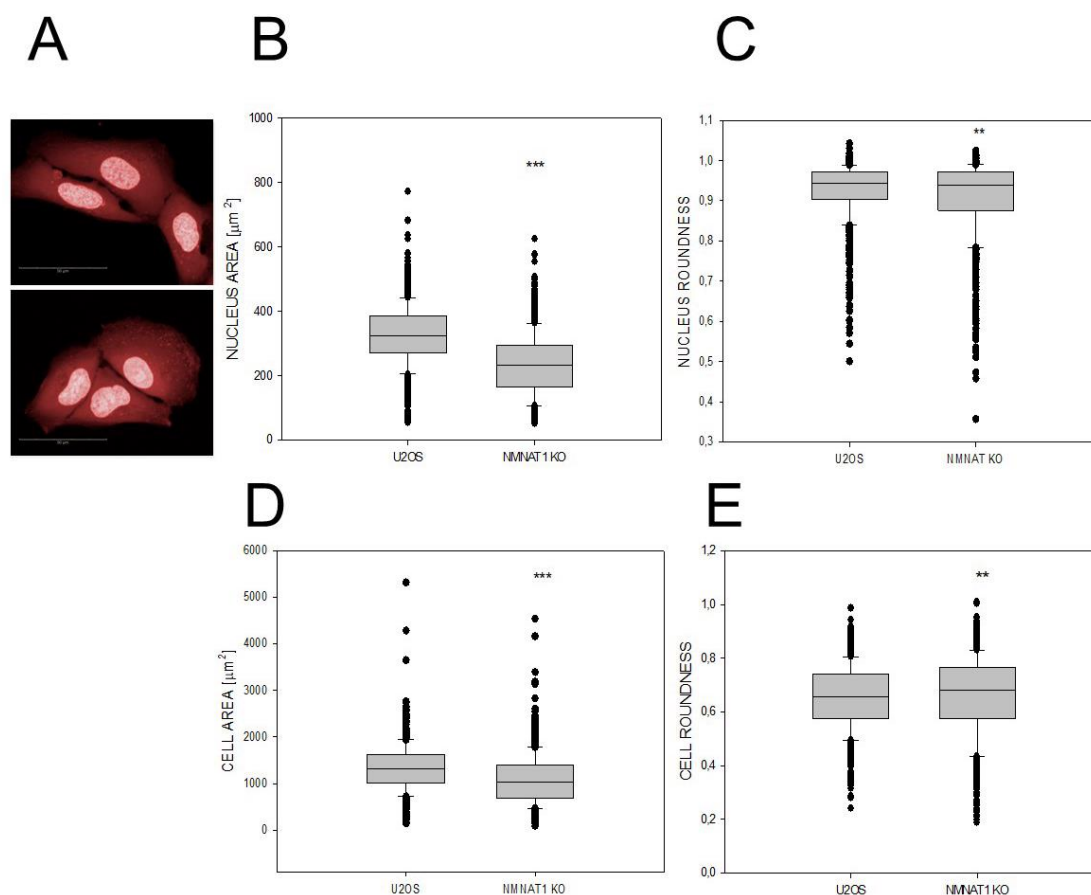


Fig 5. Morphological properties of wild type and NMNAT1 knockout cells

Cells were stained with Draq5 live cell dye. Images were taken with Opera Phoenix High Content Analyzer (A). Image analysis was performed to explore morphological differences (nuclear area: B; nuclear roundness: C; cell area: D and cell roundness: E) between the two cell lines. Data is expressed in means \pm SEM ($n = 3$). * $P < 0.05$; ** $P < 0.01$; *** $P < 0.001$.

NMNAT1 knockout cells have decreased basal total NAD levels (Fig 6A), but no significant difference was found in the regarding ATP content (Fig 6B). Parameters of basal energy metabolism were also investigated with Seahorse metabolic analyzer. No significant change could be detected in oxygen consumption rate (OCR) between the two cell lines (Fig 6C). Extracellular acidification rate (ECAR) showed a marked elevation in the KO cells (Fig 6D).

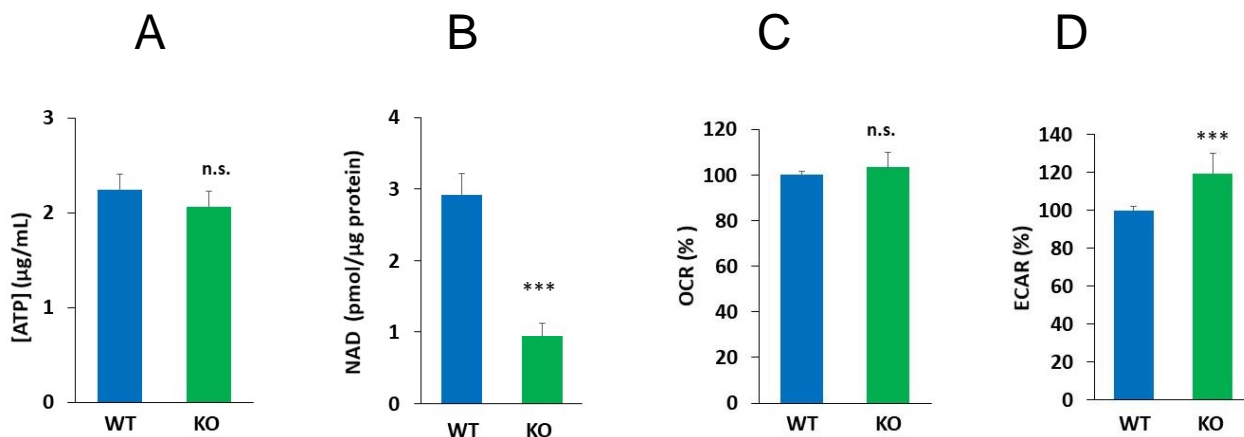


Fig 6. Characterization of the NMNAT1 KO cell line: metabolic parameters

Basal total NAD (A) and ATP (B) levels were assayed from cell lysates and normalized to protein content. Seahorse metabolic analyzer was used to determine the activities of basal metabolic routes, oxidative phosphorylation (Oxygen consumption rate, C) and glycolysis (extracellular acidification rate, D). Plotted are means \pm SEM (n = 3). *P < 0.05; **P < 0.01; ***P < 0.001.

Cisplatin is used in the base therapy of osteosarcoma [10]. Chemosensitivity of wild type and NMNAT1 KO U2OS cells was compared in a calcein AM viability assay, with a concentration series of cisplatin, ranging between 0.725-10 μ g/mL (Fig 7A). Knockout cells proved to be significantly more sensitive to the treatment, than their wild type counterparts. The mode of action of cisplatin includes DNA damage [11], which can be followed by the detection of the phosphorylation of H2AX at Ser 139 (γ -H2AX) [12] which correlates with DSB. Immunocytochemistry was followed by high content analysis, to determine morphological changes (Fig 7B). Three groups (normal, spotted, fragmented) of cell morphology was determined. The ratio of H2AX focus containing (spotted) cells was significantly increased in both cell lines, while the ratio of fragmented morphology was increased only in the KO cells, which may reflect an inadequate DNA repair ability.

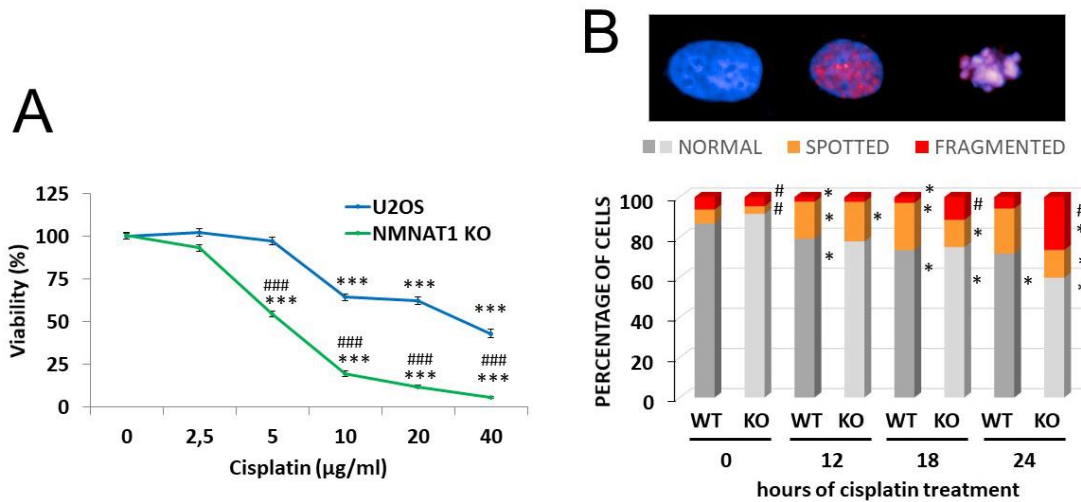


Fig 7. Assay of viability and DNA repair after cisplatin treatment

Chemosensitivity of wild type and knockout cells was first compared in a Calcein-AM viability assay after 24 hours of treatments with different concentrations of cisplatin (6.25-10 µg/mL) (A). Cisplatin-induced DNA damage was followed with an analysis of P-H2AX signal with immunocytochemistry. High content analysis detected three different cell morphologies: “normal” cells contain no P-H2AX signal, “spotted” cell type contain P-H2AX foci, while “fragmented” type shows a condensed morphology, with a diffuse P-H2AX signal, representative images of the three morphologies are shown (B). Chart shows the percentage of the three types of morphologies in control, 12, 18 or 24 hour of cisplatin treatment (B). Error bars are not shown on panel B because of the 3D representation. Data is expressed in means ± SEM (n = 3). *P < 0.05; **P < 0.01; ***P < 0.001.

Apoptotic cell death is mediated by caspases. A fluorescent, caspase-3/8 specific substrate was used to assay caspase activity. Fluorescent images were taken (Fig 8A) and analyzed (Fig 8B) by Perkin Elmer Opera Phoenix High Content analyzer in a live cell containing kinetic assay. Caspase activity was assayed between 12-22 hours after cisplatin treatment. Images were taken in every hours. Representative images (Fig 8A) show the caspase positivity at 22h. Image analysis lead to express the percentage of caspase+ cells is shown, compared to the total number of cells (Fig 8B). A low level (~2%) of spontaneous apoptosis is found in both WT and KO cells without treatment. Cisplatin caused a significant caspase activation at the KO cell line, starting at 15h. Caspase positivity is lower at WT cells, elevates much lower and only after 20 hours of cisplatin treatment. Number of caspase+ cells could be significantly decreased by the DEVD-FMK caspase inhibitor (Fig 8B). Elevation of level of lactate dehydrogenase in the supernatant is an indication of necrotic/necroptotic cell death. Cisplatin treatment resulted in a marked elevation of LDH in the case of the KO cell line, which could be prevented by a pretreatment of the necroptosis inhibitor, NEC1 (Fig 8C).

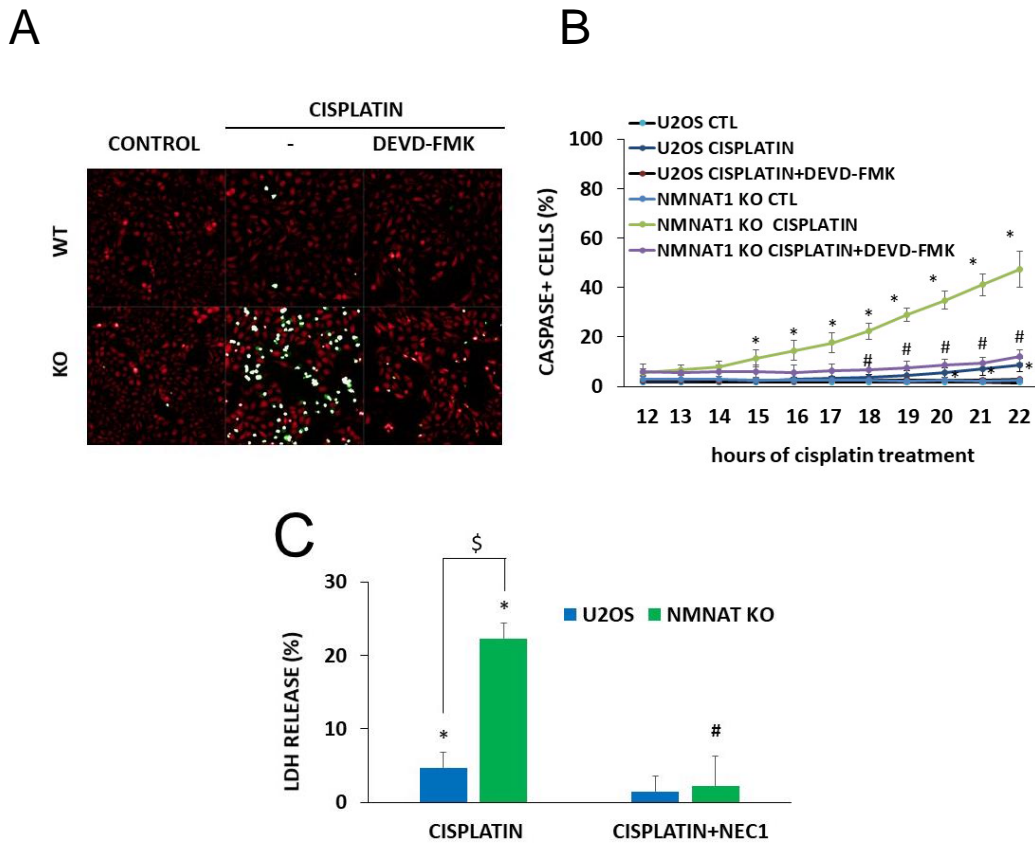


Fig 8. Assay of apoptotic and necroptotic cell death

Apoptotic cell death was followed by the detection of a fluorogenic caspase-3 substrate in a kinetic assay in an incubated in a High Content Analyzer. Representative images (A) show the signal of the caspase substrate (green signal) with a digital phase contrast (red signal) at 22 hours after cisplatin treatment. Cisplatin was used alone, or in a combination with a caspase-3 inhibitor, DEVD-FMK. Images were taken in every hours, between 12-22 hours of, and analyzed for the number of caspase+ cells, as a percentage of the actual number of cells (B). LDH release was determined from the supernatants, after 24 hours of cisplatin treatment, and expressed as a percentage of the positive control (lysed cells). Cells were treated with cisplatin or with the combination of cisplatin with the necroptosis inhibitor, necrostatin-1 (NEC1) (C). Data is expressed in means \pm SEM (n = 3). *P < 0.05; **P < 0.01; ***P < 0.001.

In the next part of our recent work, metabolic parameters were assayed in the presence of cisplatin. Total cellular NAD⁺ content was measured after 24 hours of cisplatin treatment (Fig 9A). The significantly lower basal NAD level in the KO cells was further decreased upon cisplatin treatment, while there was no significant change in the wild type cells. Cisplatin treatment resulted in a significantly decreased cellular ATP level in the knockout cells (Fig 9B), where the drop in ATP level could be decreased by pretreatments with both apoptosis and necroptosis inhibitors. In the wild type cells, no significant change was detected at any treatments.

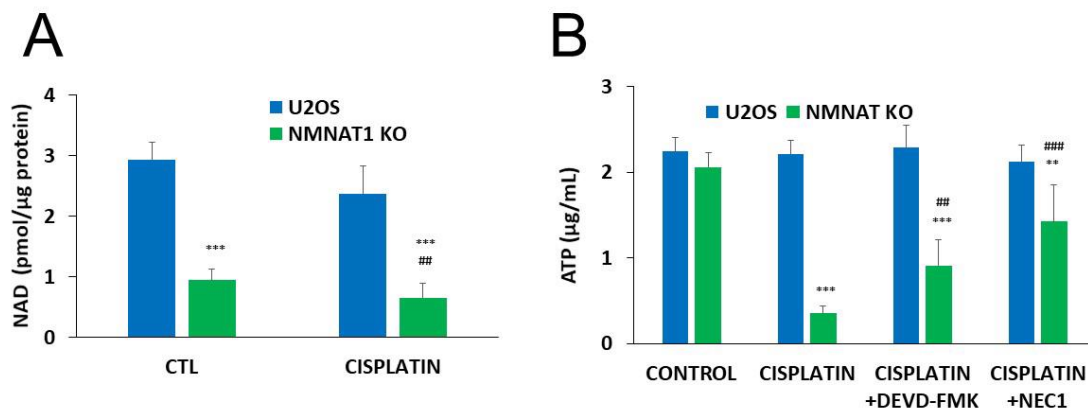


Fig 9. Measurement of alterations in NAD and ATP content after cisplatin treatment
 After 24 hours of cisplatin treatment total NAD levels were determined in WT and KO cells from cell lysates and normalized to protein content (A). Cellular ATP were assayed 24 hours after cisplatin treatment, cells were treated with cisplatin alone or in a combination with apoptosis (DEVD-FMK) or necroptosis (NEC1) inhibitors (B). Data is expressed in means \pm SEM (n = 3). *P < 0.05; **P < 0.01; ***P < 0.001.

Seahorse metabolic analyzer is capable for the detection of both oxidative and glycolytic metabolism. There is no difference in the basal oxygen consumption rate (OCR) between the two cell lines (Fig 10A), cisplatin treatment alone caused a similar, decreased OCR on the both cell lines. However, mitochondrial stress test reveals a huge difference in the adaptation properties of cisplatin treated KO cell line (Fig 10A). Basal extracellular acidification rate (ECAR), which reflects glycolytic activity proved to be significantly higher in the KO cell line (Fig 10B). ECAR have shown no significant change after 13 hours of cisplatin treatment, compared to the non-treated controls. Glycolytic stress test could be passed even after cisplatin treatment (Fig 10C).

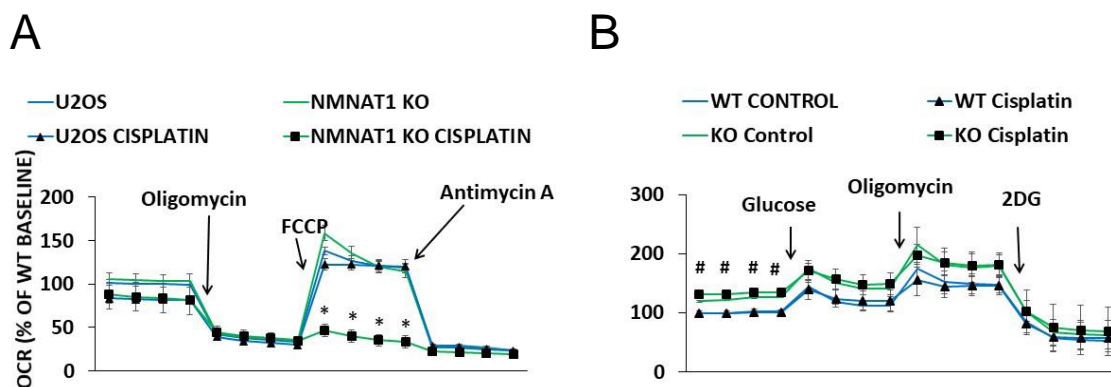


Fig 10. The effect of cisplatin on routes of energy metabolism
 OCR/oxidative phosphorylation (A) and ECAR/glycolytic activity (B), was measured with Seahorse metabolic analyzer (Agilent). Both parameters was followed during specific stress tests, 13 hours after cisplatin treatment (in vehicle and cisplatin treated samples as well). Mitochondrial stress test includes oligomycin, FCCP and antimycin A (A); Glycolysis stress test utilizes glucose, oligomycin and 2-deoxyglucose (B).

PARP1 enzyme is activated by sensing DNA damage [13], to help DNA repair processes. As the polymers are synthesized from NAD⁺, it was hypothesized that decreased NAD may cause at least a partial inhibition of PARP1 enzyme. The activity of PARPs can be indirectly measured by the detection of poly(ADP-ribose) polymers. Cisplatin caused a

time dependent PAR formation in WT cells (Fig 11A, B), while, a no significant polymer formation could be detected in the KO cells. Inhibition of PARP1 is reported to cause a decreased proliferation rate [14]. The effect of PARP inhibition was compared to the NMNAT1 KO phenotype on proliferation (Fig 11C). Cisplatin treatment caused a significant reduction in the clonogenic activity of NMNAT1 KO cells. Wild type cells have shown no significant decrease in clonogenic activity for cisplatin treated samples. The combination of cisplatin with a PARP inhibitor (olaparib) treatment caused a significantly lower proliferation in wild type cells, but no further decrease could be detected in the KO cells (Fig 11C).

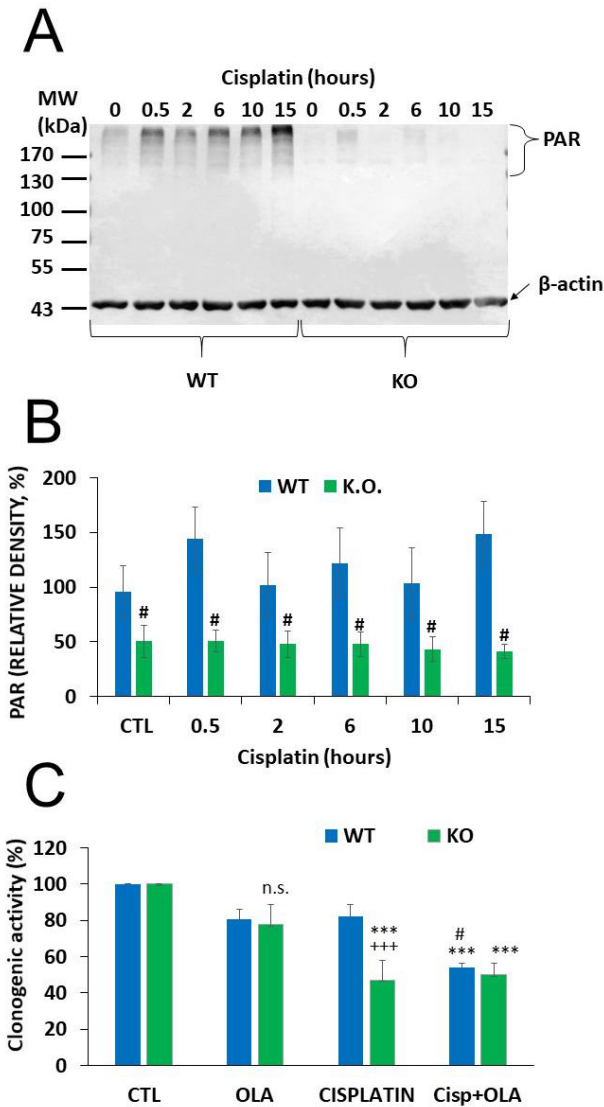


Fig 11. PARP inhibition is partially responsible for the sensitizing effect of NMNAT1 depletion The level of PAR polymers was detected in wild type and in NMNAT1 KO cells at different time points (0.5h, 2h, 6h, 10h and 15h) after cisplatin treatment with western blot (A). Beta-actin was used as a loading control. Relative densities (normalized to beta actin and compared to the untreated control of WT cell line) are shown (B). The role of possible of PARP-1 - NMNAT1 interaction in clonogenic activity was determined in a conventional clonogenic assay, (6 days) (C). Cells were treated with vehicle (CTL), cisplatin or the combination of cisplatin and olaparib (Cisp+OLA). Individual colonies were counted in each samples, results are expressed as percentages, compared to the number of colonies in the untreated samples. Data is expressed in means ± SEM (n = 3). *P < 0.05; **P < 0.01; ***P < 0.001.

3D cultures can be better models of *in vivo* conditions, a 3D model of chemosensitization to cisplatin by NMNAT1 deficiency was also set. Wild type and NMNAT1 KO U-2OS cells formed spheroids in a similar way. However, cell-to-cell contacts in spheroids make cells more resistant to toxic stimuli [15] therefore, we used higher concentrations of cisplatin in the spheroid experiments (50 $\mu\text{g}/\text{mL}$). While spheroids of the wild type cells only became less compact at cisplatin concentration, NMNAT1 KO U-2OS cells displayed a significant decrease in size, or a completely disintegrated (Fig 12A, B). The inner region of cisplatin treated spheroids show an elevation in Annexin V positivity, a more dramatic elevation could be detected in NMNAT1 KO spheroids (Fig 12C).

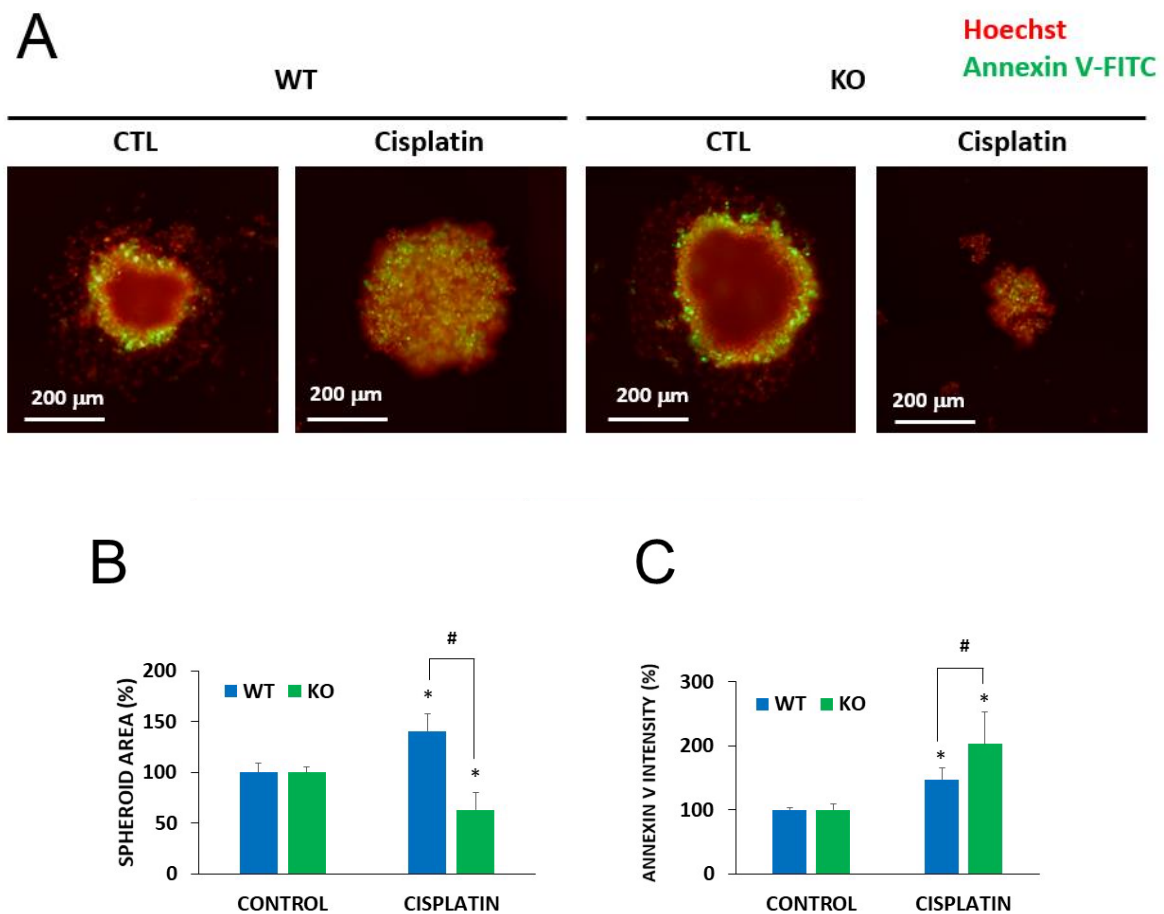


Fig 12. 3D chemosensitivity model

WT and KO cells were seeded on agarose coated, U-shaped wells of 96 well plates to form spheroids. Spheroids were treated with 50 $\mu\text{g}/\text{mL}$ cisplatin for six days. Images were taken (A) and analyzed for size (B) and the intensity of Annexin V in the inner sections of the spheroids (C) Data is expressed in means \pm SEM (n = 3). *P < 0.05; **P < 0.01; ***P < 0.001.

In the base therapy of osteosarcoma, cytotoxic agents are often used in combination. At first, we set up a doxorubicin concentration, to find a monotherapy dose, which may cause a high toxicity at least in the KO cells (Fig 13A). The effect of cisplatin on viability was measured in combination with doxorubicin. With a constant concentration of doxorubicin, (which was much lower than in the monotherapy experiments) and increasing concentration of cisplatin (Fig 13B). A significantly higher sensitivity could be detected in the case of NMNAT1 KO clones. The two drugs acted synergistically, and a concentration dependent manner (Fig 13B). The effective concentrations of both drugs could be lowered compared to the concentration which was effective in monotherapy.

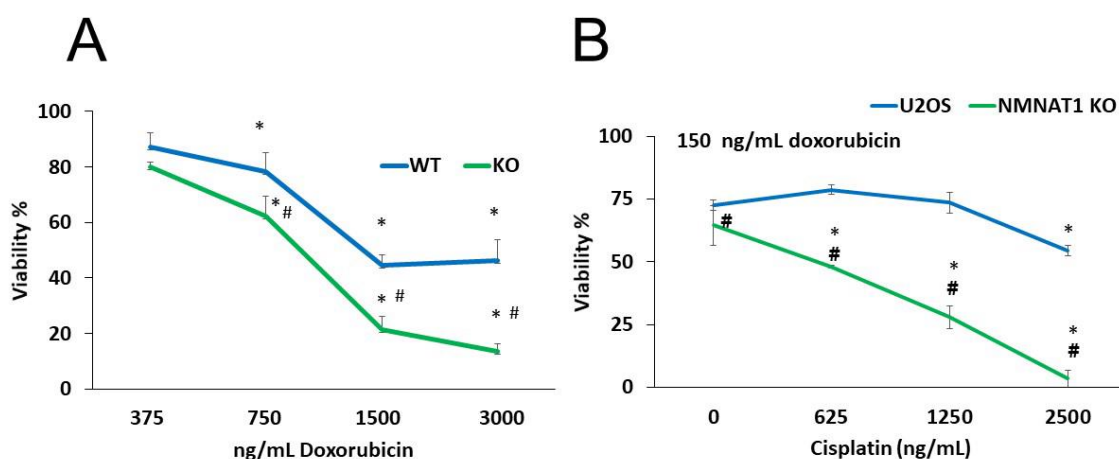


Fig 13. The effect of doxorubicin and combined chemotherapy treatments on viability

Calcein-AM viability assay was performed after 24 hours treatments with different concentrations of doxorubicin on wild type and NMNAT-1 KO cells (A). Testing of chemosensitivity was also performed by using combined treatments with a constant concentration of doxorubicin and increasing concentrations of cisplatin (B). Data is expressed in means \pm SEM (n = 3). *P < 0.05; **P < 0.01; ***P < 0.001.

Sensitizing effect of NMNAT-1 silencing to cisplatin induced cytotoxicity was also tested in SAOS-2 human osteosarcoma cells. SAOS-2 cells could be effectively silenced (Fig 14B). Similarly to NMNAT-1 knockout U-2OS cells, NMNAT-1 silenced SAOS-2 cells showed significantly higher sensitivity to cisplatin treatment (Fig 14A).

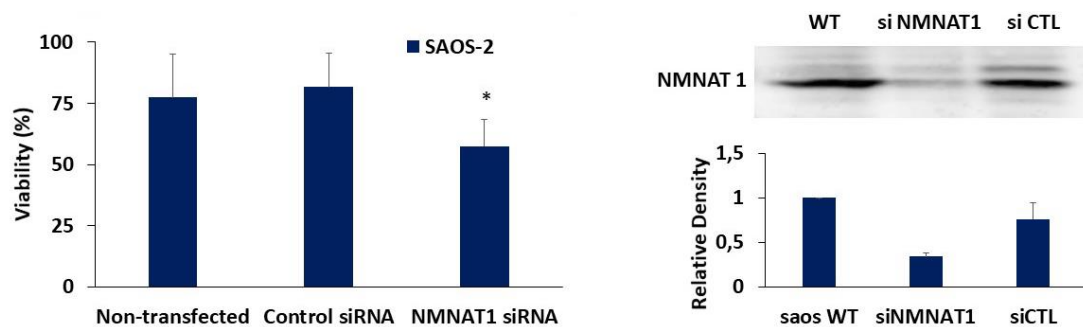


Fig 14. SAOS-2 chemosensitivity model

Saos-2 cells were transfected with control or NMNAT-1 specific siRNAs. Cells were treated with cisplatin for 48 hours and a calcein-AM viability assay was performed (A). Proof of NMNAT1 silencing on SAOS-2 cells is shown on panel B. Data is expressed in means \pm SEM (n = 3). *P < 0.05; **P < 0.01; ***P < 0.001.

Summary

We found that U-2OS human osteosarcoma cells tolerate the genetic inactivation of the NMNAT1 gene, no major morphological differences were found between the WT and KO cells. However, elimination of NMNAT1 protein caused a decrease in proliferation and NAD-content and increased glycolytic activity, viability and ATP levels and the rate of oxidative phosphorylation remained unchanged. NMNAT1 KO U2OS cells show increased sensitivity to cisplatin and doxorubicin. Chemosensitivity of the NMNAT1^{-/-} phenotype is due in part to restricted DNA-damage-induced protein PARylation and consequently enhanced DNA damage. U-2OS cells unable to respond sufficiently to cisplatin treatment undergo caspase-mediated apoptotic and caspase-independent necroptotic death. Cisplatin treatment caused dramatic decrease in cellular ATP levels and in the mitochondrial reserve respiratory capacity, neither could be seen in the wild type cells. Increased chemosensitivity was also confirmed on another osteosarcoma cell line and in a 3D model, suggesting that NMNAT1 may be worth investigating further as a potential target in cancer therapy with special regard to osteosarcoma treatment.

The manuscript based on our recent work was submitted to Cellular and Molecular Life Sciences (CMLS) as follows: Alexandra Kiss, Arnold Péter Ráduly, Zsolt Regdon, Zsuzsanna Polgár, Szabolcs Tarapcsák, Isotta Sturniolo, Tarek El-Hamoly, László Virág, Csaba Hegedűs : Targeting nuclear NAD synthesis increases chemosensitivity of U-2OS osteosarcoma cells by suppressing poly(ADP-ribosyl)ation-dependent DNA repair and impaired metabolic adaptation

References

1. Pavlova, N.N. and C.B. Thompson. The Emerging Hallmarks of Cancer Metabolism. *Cell Metab* **2016**. *23(1)*: p. 27-47.
2. Kim, M.Y., T. Zhang, and W.L. Kraus. Poly(ADP-ribosyl)ation by PARP-1: 'PAR-laying' NAD⁺ into a nuclear signal. *Genes Dev* **2005**. *19(17)*: p. 1951-67.
3. Burkle, A. and L. Virag. Poly(ADP-ribose): PARadigms and PARadoxes. *Mol Aspects Med* **2013**. *34(6)*: p. 1046-65.
4. Farmer, H., N. McCabe, C.J. Lord, A.N. Tutt, D.A. Johnson, T.B. Richardson, M. Santarosa, K.J. Dillon, I. Hickson, C. Knights, N.M. Martin, S.P. Jackson, G.C. Smith, and A. Ashworth. Targeting the DNA repair defect in BRCA mutant cells as a therapeutic strategy. *Nature* **2005**. *434(7035)*: p. 917-21.
5. Guo, Q., N. Han, L. Shi, L. Yang, X. Zhang, Y. Zhou, S. Yu, and M. Zhang. NAMPT: A potential prognostic and therapeutic biomarker in patients with glioblastoma. *Oncol Rep* **2019**. *42(3)*: p. 963-972.
6. Barraud, M., J. Garnier, C. Loncle, O. Gayet, C. Lequeue, S. Vasseur, B. Bian, P. Duconseil, M. Gilabert, M. Bigonnet, A. Maignan, V. Moutardier, S. Garcia, O. Turrini, J.R. Delpero, M. Giovannini, P. Grandval, M. Gasmi, M. Ouaiissi, V. Secq, F. Poizat, N. Guibert, J. Iovanna, and N. Dusetti. A pancreatic ductal adenocarcinoma subpopulation is sensitive to FK866, an inhibitor of NAMPT. *Oncotarget* **2016**. *7(33)*: p. 53783-53796.
7. Song, T., L. Yang, N. Kabra, L. Chen, J. Koomen, E.B. Haura, and J. Chen. The NAD⁺ synthesis enzyme nicotinamide mononucleotide adenylyltransferase (NMNAT1) regulates ribosomal RNA transcription. *J Biol Chem* **2013**. *288(29)*: p. 20908-17.
8. Zhang, T., J.G. Berrocal, J. Yao, M.E. DuMond, R. Krishnakumar, D.D. Ruhl, K.W. Ryu, M.J. Gamble, and W.L. Kraus. Regulation of poly(ADP-ribose) polymerase-1-dependent gene expression through promoter-directed recruitment of a nuclear NAD⁺ synthase. *J Biol Chem* **2012**. *287(15)*: p. 12405-16.
9. Yaku, K., K. Okabe, and T. Nakagawa. NAD metabolism: Implications in aging and longevity. *Ageing Res Rev* **2018**. *47*: p. 1-17.
10. Chuang, V.P., S. Wallace, R.S. Benjamin, N. Jaffe, A. Ayala, J. Murray, J. Zornoza, Y. Patt, G. Mavligit, C. Charnsangavej, and C.S. Soo. The therapy of osteosarcoma by intraarterial cis-platinum an limb preservation. *Cardiovasc Intervent Radiol* **1981**. *4(4)*: p. 229-35.
11. Turchi, J.J., K.M. Henkels, I.L. Hermanson, and S.M. Patrick. Interactions of mammalian proteins with cisplatin-damaged DNA. *J Inorg Biochem* **1999**. *77(1-2)*: p. 83-7.
12. Zhao, H., X. Huang, H.D. Halicka, and Z. Darzynkiewicz. Detection of Histone H2AX Phosphorylation on Ser-139 as an Indicator of DNA Damage. *Curr Protoc Cytom* **2019**. *89(1)*: p. e55.
13. Hegedus, C. and L. Virag. Inputs and outputs of poly(ADP-ribosyl)ation: Relevance to oxidative stress. *Redox Biol* **2014**. *2*: p. 978-82.
14. Wang, Z., Y. Li, S. Lv, and Y. Tian. Inhibition of proliferation and invasiveness of ovarian cancer C13* cells by a poly(ADP-ribose) polymerase inhibitor and the role of nuclear factor-kappaB. *J Int Med Res* **2013**. *41(5)*: p. 1577-85.
15. Baek, N., O.W. Seo, J. Lee, J. Hulme, and S.S. An. Real-time monitoring of cisplatin cytotoxicity on three-dimensional spheroid tumor cells. *Drug Des Devel Ther* **2016**. *10*: p. 2155-65.